18th Brazilian Congress of Thermal Sciences and Engineering
November 16-20, 2020 (Online)

ENC-2020-0365
CHARACTERIZATION OF THE FIRST COMBUSTION CYCLES OPERATING ON SI ENGINE WITH PFI, LATERAL AND CENTRAL DI FOR GASOLINE-ETHANOL AND GASOLINE FUEL

Maycon F Silva
Pedro Teixeira Lacava
Technological Institute of Aeronautics, Laboratory of Combustion, Propulsion and Energy, São José dos Campos, SP, Brazil
mayconfsilva@yahoo.com.br, placava@ita.br

Abstract. *Due to the difficulties in the first combustion cycles, providing ignition failures, and unstable combustion, a better understanding of the flame propagation behavior in this period was sought. With the aid of a research engine with optical access, the characteristics of the first cycles were investigated from the port fuel injection, lateral and central direct injection modes, being fed with gasoline and the gasoline-ethanol mixture. With the engine operated at a speed of 900 rpm for analysis of combustion behavior with low turbulent effects, optical and thermodynamic data were obtained. The results for port fuel injection suggest an increase in the flame area as the operation cycles increase, providing also a decrease in flame deformation. The absence of flame at the beginning of the process was observed, followed by unstable combustion. For the lateral direct injection mode, combustion achieved results close to the permanent thermal regime from the beginning, however, it presents great variability. The change of position to central direct injection showed improvements in the fuel distribution within the chamber, providing results with more speed and less variability. The increase in injection pressure also showed satisfactory results, thus proving to be an excellent technique to overcome evaporation difficulties.*
Keywords: *Combustion, First Cycles, SI Engines, Ethanol, Gasoline, Direct Injection, Port Fuel Injection.*

1. INTRODUCTION

Over the past century, internal combustion engines have been the main source of energy in the transportation sector due to their low cost, good performance in some applications, high reliability, and potential for operation with various types of fuels (Aleiferis et al, 2004). However, internal combustion engines face global agreements with strict legislation relating to both the reduction of pollutant emissions and energy efficiency.

In the last decade, due to pollution regulations, much attention has been given to biofuels. Ethanol has been identified as one of the most important to address these issues due to its physical and chemical properties and its ability to be used as a complete and partial substitute for gasoline. Among the main properties, lower emission of pollutant gases, high octane rating, and lower production cost of ethanol compared to gasoline (Awad, 2018). Due to its properties, several authors have shown that adding ethanol to gasoline could improve burning rates and overall efficiency due to its high combustion speed (Zhuang, 2013 Baeta, 2015 and Shahad, 2015). In addition, the high octane number and high latent heat of ethanol vaporization allow higher engine compression rates which would improve the thermal efficiency of the ethanol-gasoline blend (Yang 2015 and WaQas 2016).

Even though the use of ethanol as an additive or substitute (partial or complete) for gasoline has been extensively studied in port fuel injection (PFI) and direct injection (DI) modes, these studies are focused on combustion analysis and engine performance under stable operating conditions (Augoye et. al., 2015; Costa et al., 2015; Di Iorio, et al., 2015 and Trevas et al., 2017). Few works are dedicated to the investigation of the cold start regime in an SI engine powered with a high percentage of ethanol (Romero et al., 2016 and Kumar et al., 2017), where due to its characteristics, the fuel presents great combustion instability (Fan et. al., 2013 and Zhang et al., 2017). To overcome this initial period, fuel-rich injection is applied several times to ensure ignition, however, excess fuel and inefficient catalytic converter operation in this period are responsible for high levels of HC and CO emissions.

Thus, the study of the behavior of the first combustion cycles is of great importance for ignition engines, regardless of the injection mode applied (Heywood, 1988 and Fan et. al. 2013), where the great instabilities of these cycles concerning subsequent cycles determine high levels of emissions and low efficiency in the combustion process, negatively affecting engine performance.

To minimize project modifications and bring solutions to low-temperature firing problems, a deeper understanding of the combustion process in the first cycles is needed. With this, the work aims to investigate the beginning and propagation of combustion in an optical internal combustion engine powered by the commercial gasoline-ethanol blend

G73E27 (73% gasoline and 27% ethanol) compared to pure gasoline (G100), where optical and thermodynamic data are analyzed.

2. EXPERIMENTAL PROCEDURE

To perform the tests, an AVL 5406 spark-ignition internal combustion engine with optical access, active AC dynamometer, acquisition system, and control unit was used. From its specifications, the AVL 5406 4-valve engine (2 intakes and 2 exhausts), has a total volume of 530 cm^3, crankshaft 144 mm, engine stroke 90 mm, and piston diameter 82 mm.

The quartz combustion chamber and the 72 mm diameter fused silica window attached to the piston crown allow optical access to the interior. With the aid of an appropriate mirror inclined at 45° fixed to the bottom of the elongated piston and the radiation produced by combustion within the chamber, images can be recorded by the acquisition system. The system configuration allows access to 64 mm in diameter. The experimental apparatus and the image acquisition scheme used are shown in Figure 1.

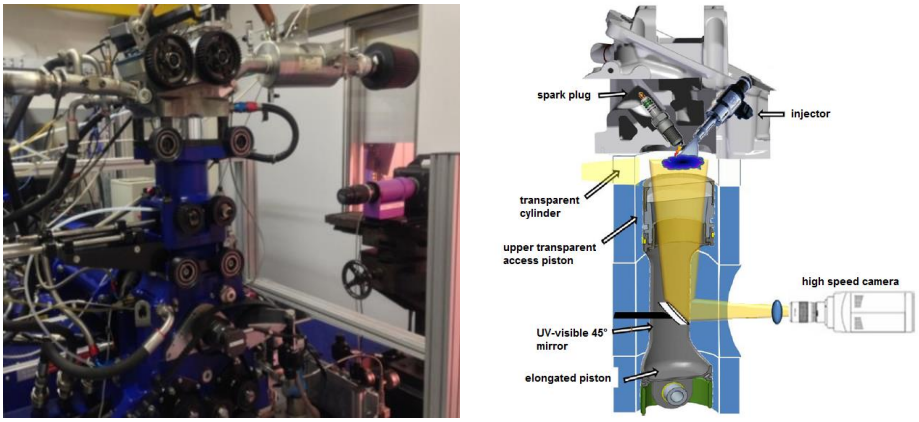

Figure 1. Experimental apparatus with AVL 5406 motor and high-speed camera and scheme of the experimental apparatus (Adapted from: (Catapano, et al. 2013).

A high-speed PCO.Dimax S1 camera coupled with a VS4-1845HS Scope dual intensifier and 105 f/4.5 UV-Nikon lenses were used to obtain optical data. A region of interest of 864x896 pixels, the frame rate of 5400 fps, corresponding to 1 image for each crank angle (CA) at 900 rpm, was selected.

The optical configuration made it possible to detect image sequences with a resolution of 91 μm/pixel. For a more complete investigation of the first combustion cycles, the tests consisted of acquiring 62 frames per cycle during the initial 80 cycles after the injection moment. Figure 2 shows the view obtained by the high-speed camera from the top of the cylinder. The possible positions for the DI injector (lateral or central) are shown in Figure 2. The spark plug is located 5mm above the geometric center of the chamber.

The engine was adjusted with a rotation speed of 900 rpm and barometric intake pressure of -19 mbar (load of 25%), where the parameters were adjusted to optimize the combustion process at the point of MBT (Maximum Brake Torque) in stationary operation. It was used at the beginning of the injection at 290°CA BTDC (Before Top Dead Center) for both lateral and central DI and 295°CA ATDC (After Top Dead Center) for PFI. For the PFI tests, to obtain the MBT, the fuel injection gauge pressure of 4.2 bar and ignition advance of 06°CA BTDC for G73E27 and 0°CA BTDC for G100, were used. For DI in the lateral position, 150 bar injection gauge pressure and 8°CA BTDC ignition advance for G73E27 and 4°CA BTDC for G100. For the central position DI tests, 150 and 200 bar fuel injection and 2°CA BTDC ignition advance for both injection pressures for the G73E27 were performed.

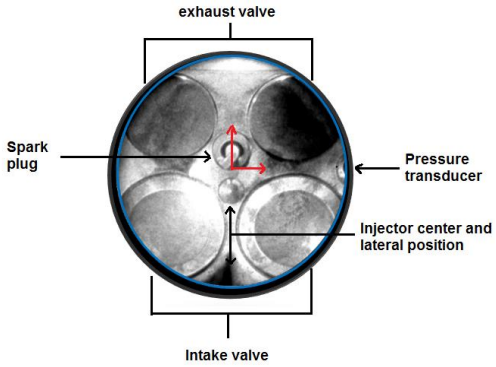

Figure 2. Combustion chamber geometry, with intake and exhaust valves, spark plug and pressure transducer.

2.2. Testing procedure

Before the start of the tests, the room where the dynamometer is located was conditioned to a temperature of 16°C. For each experimental test performed, with the parameters of those already selected, the operation of the engine without combustion (motorized) was started at the selected speed and load. Upon reaching this condition, the high-speed camera and fuel injection were triggered, thus starting the combustion process. After the process was completed, the injection was stopped and the engine was switched off. For a minimum period of 15 min, the engine was kept off under a controlled temperature of 16°C to accelerate its cooling. As a dynamometer safety measure, the engine keeps the coolant and lubricating oil warm at 60°C.

2.3. Image processing

To obtain quantitative data and a geometrical representation of the flame, a processing was developed with the help of the Vision of National Instruments program (Vision Assistant 2016, NI – Academic license, Austin, Texas, EUA). With the software for image processing (Figure 3), the intensity plane was extracted and spurious (reflections and lights around the optical access) were corrected. After that, with the binarized image, the appropriate threshold was set from the Clustering method, which presented the most precise definition of the flame area. Once the effective area in pixel was calculated, the scale adjustment was used to obtain the morphology parameters in unit of the international system.

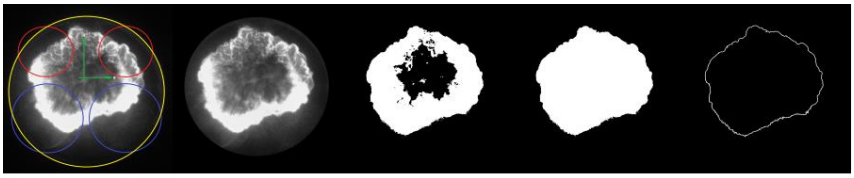

Figure 3. Image processing. (a) Original photographic record in 8 bits. (b) Circle mask applied. (c) Threshold application and image binarization. (d) Fill in gaps. (e) Analyzed flame edge.

3. RESULTS

To better understand the behavior and operating conditions of the internal combustion engine in the first combustion cycles, images from the first 30 cycles were taken with the help of the high-speed camera. Well-defined characteristics are observed in figure 4 for both fuels in PFI operation mode. In the images, it was possible to observe the absence of the flame in the initial cycles for both fuels (4th cycle for G73E27 and 3rd cycle for G100). After this initial period, the flames appear, however still showing great variability, low illumination and a growth still far from reaching the optical limit. As the flame combustion process progresses, it tends to show stronger illumination and more satisfactory growth in later cycles.

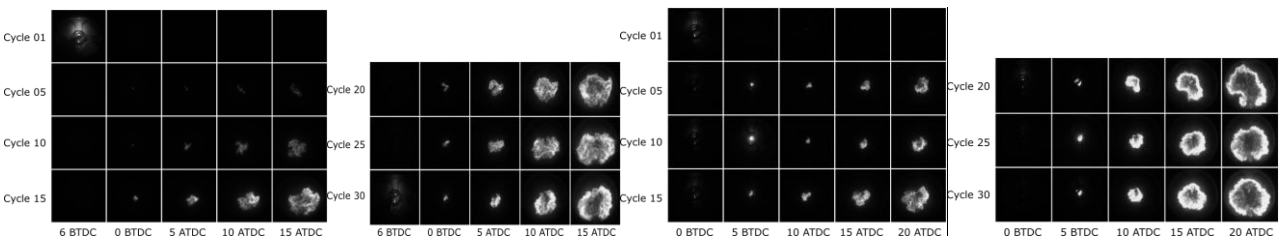

Figure 4. Flame propagation sequences after ignition of cycles 01 to 30 by the PFI mode for G73E27 and E100.

For the same purpose as the images acquired in the PFI, the same procedure was performed for the DI mode. Contrary to the results visualized in the PFI, the photographic records (Figure 5) of the DI showed well developed flame formation since the first cycles of operation. Despite the faster combustion response of the first operating cycles, ignition failures and great variability in flame behaviour are common during this initial period. Despite cyclic variability and intensity variations, unlike PFI mode, direct injection provided flame ignition and propagation in all cycles. As the combustion process progresses, it can be seen that more uniformity in flame propagation is obtained.

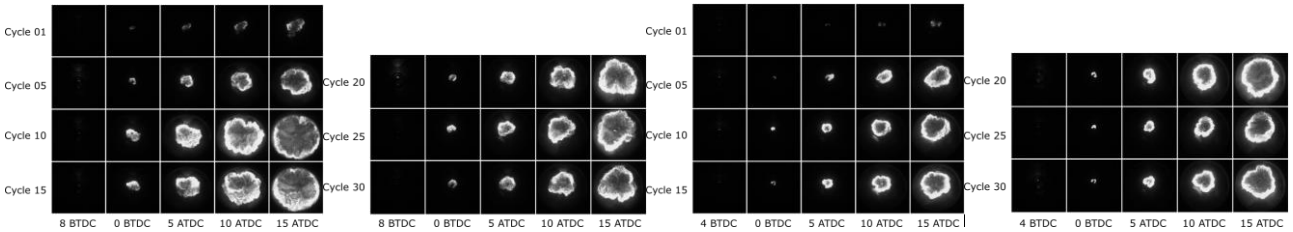

Figure 5. Flame propagation sequences after ignition of cycles 01 to 30 by the lateral DI mode for G73E27 and E100.

From the sequences of propagation images obtained, the evolution of the flame area was calculated. As shown in Figure 6, it is possible to see that with the progress of the operation, the flame tends to develop better and thus has a better speed of propagation. This behavior has a direct influence on the slope of the curve, thus bringing the cycles closer and closer to the curve obtained in a permanent thermal regime (PTR).

The presence of ethanol in G73E27 may interfere with the chemical characteristics of the fuel such as the latent heat of vaporization. This feature can provide greater difficulty in vaporization especially at the beginning of operation due to the low temperature of both the fuel and the engine and its parts. This difficulty can lead to less flame development, greater variability, and absence of flame in some cases.

Far from PTR, the low development of G100 is due to the evolution of the burning and the value of the air-fuel ratio in the studied period. Despite the higher amount of volatile compounds and heat of vaporization about 3 times lower than ethanol, difficulties of vaporization were observed and forming a poor mixture, far from the stoichiometric ideal. The observed behavior may be linked to the theoretical energy supply to the engine per cycle that each fuel provides. With the same rotation and air mass for the same fuels, for the same λ (air-fuel ratio) the adjustment of the amount of injected fuel causes different theoretical energy release rates. Thus, with a higher air-fuel mass ratio, gasoline has less theoretical energy released than ethanol from this mode of operation used in these tests. This behavior reflects the low development of gasoline in relation to ethanol for both modes of injection.

As observed in Fig. 6, the PFI model presents initial difficulty in reaching PTR at the beginning of the operation. Due to fuel injection from the intake manifold and the low injection pressure from this mode of operation, vaporization and ignition difficulties are observed in this mode. As the engine heats up, improvement is observed in the firing.

Due to the higher injection pressure, the direct injection mode, as seen in Figure 7, shows a much more satisfactory development of the flame area in this initial period. The greater vaporization of the fuel droplets provides easier distribution and burning even in low-temperature conditions reached the beginning of the combustion process. It is observed that greater variability is observed for G73E27. This is linked to the chemical characteristic of ethanol in the fuel that needs more energy to vaporize. As the combustion process progresses, the temperature tends to increase which provides the greatest stability in the evolution of the flame.

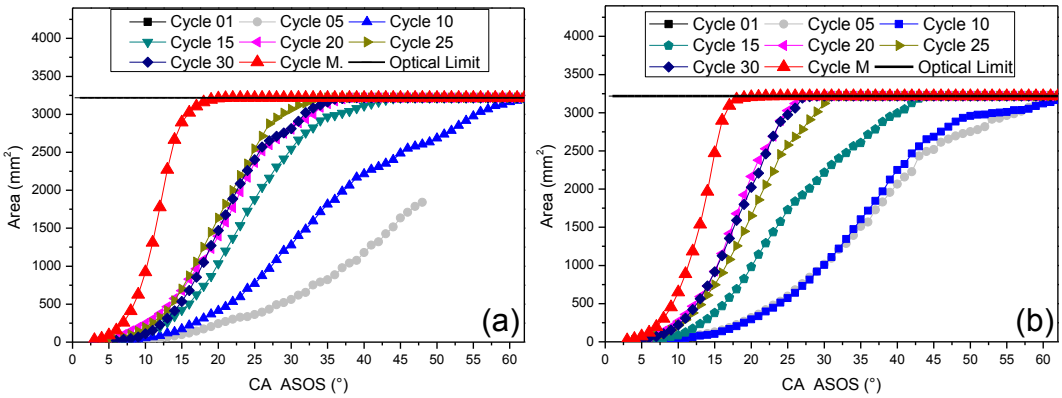

Figure 6. Area vs. Crank Angle after the start of spark (CA ASOS) by PFI for the first 30 cycles with G73E27 and G100.

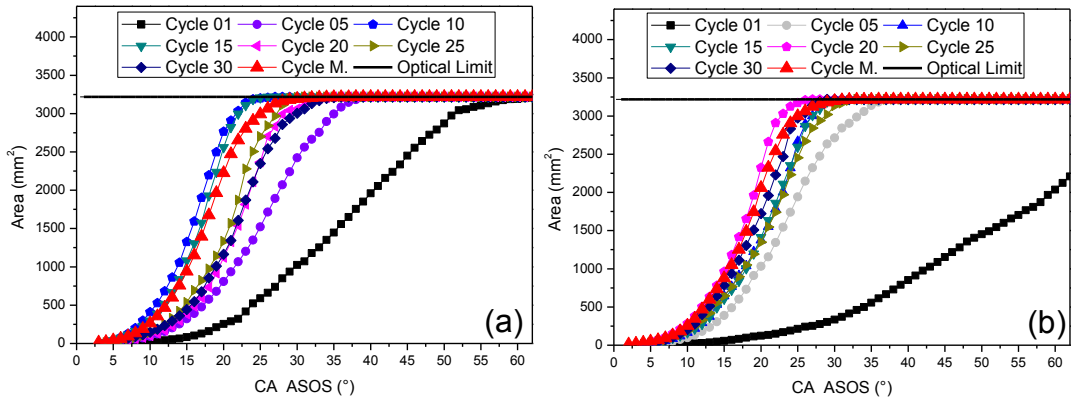

Figure 7. Area vs. Crank Angle after the start of spark (CA ASOS) by lateral DI for the first 30 cycles with G73E27 and G100.

In addition to the PFI and lateral DI modes, the characteristics of the flame were also investigated in this period of operation with different positioning of the injector and also at different pressures (150 and 200 bar). The test was performed with the G73E27 because it is the fuel sold in the country to the final consumer. Just like the lateral DI, the central DI spread has been well developed since the beginning of the process (Figure 8). Greater intensity and less variability were observed in the development of the flame area, where it was always closer to PTR compared to other injection modes. The injector located in the central region allows better distribution of the fuel within the cylinder, thus reducing the contact of the fuel mass completely direct to the wall which could cause condensation or cooling of the fuel due to the temperature of the engine parts. A significant improvement in growth and uniformity is also observed with the increase in injection pressure from 150 to 200 bar. This is due to better atomization of the fuel.

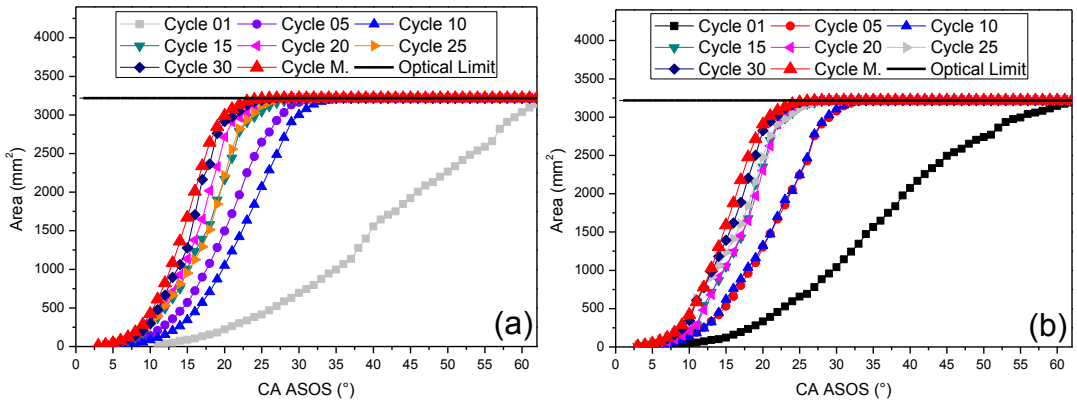

Figure 8. Area vs. Crank Angle after the start of spark (CA ASOS) by central DI for the first 30 cycles with G73E27: a)150 bar; b)200 bar.

For a more extended analysis and a better understanding of the behavior and variability of this period of operation, the crank angle was fixed and the first 80 combustion cycles were analyzed. In PFI mode (Fig. 9), exponential behavior can be observed for both fuels, thus changing only the inclination of the curve. In this injection mode, 5 stages can be observed. In the 1st stage, the low vaporization of the fuel in the intake manifold and also the low temperature in the combustion chamber provides a poor mixing ratio which induces the absence of combustion. Later, in the second stage, far from the stoichiometric period and with slight heating of the engine parts, incomplete vaporization is provided and a nucleus of the flame is observed little developed and with low luminosity. In the 3rd period, it is characterized by a considerable increase in luminosity resulting from better vaporization. Represented by a more stable condition, the fourth stage presents more stability and slight growth. In the last stage, the operation reaches the permanent thermal regime with more linear behavior and low cyclic variability. The duration of each stage will depend on the characteristics and interactions of each fuel.

Analyzing the lateral DI direct injection mode (Fig. 10), it can be seen that the evolution of the flame is always close to the average since the beginning of the operation, however, with great variability. G73E27 fuel is more affected by greater variability due to the effects of ethanol in its composition, where its characteristics provide greater resistance to vaporization at low temperatures. This behavior can provide the accumulation of fuel inside the chamber due to low temperature and difficulty to vaporize being also responsible for the high variability. After injection, due to the low temperature of the chamber wall and engine parts, heat loss from the fuel to the wall promotes less vaporization and in some cases condensation. This behavior provides less vaporized fuel at the moment of ignition and consequently a

poorer air-fuel ratio which causes incomplete combustion. In the next cycle, with the increase in temperature and pressure provided by the previous burning, the remaining fuel from the previous cycle evaporates and collaborates to the combustion process (Hattori, 1997). As the combustion process progresses, the system attempts to show more stability and variability within the standard deviation.

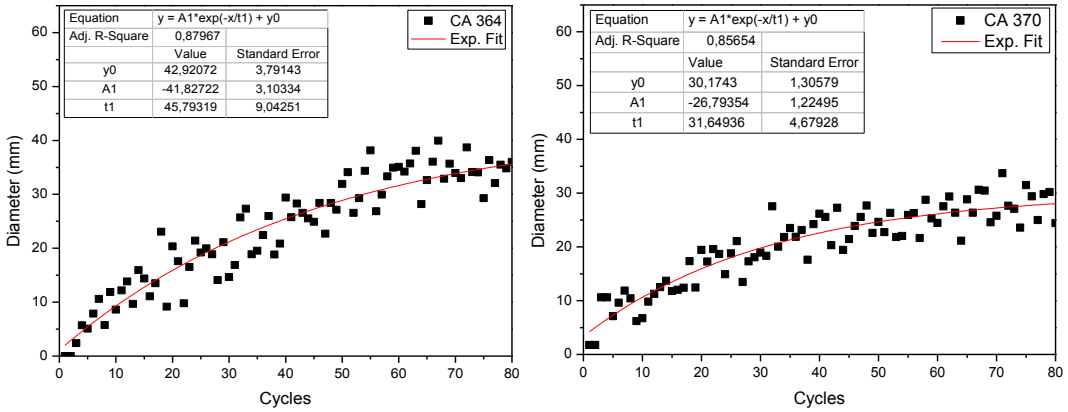

Figure 9. Diameter for the first 80 cycles of combustion versus cycles for fixed crank angle of 10 CA after ignition by PFI mode: a) G73E27; b) G100.

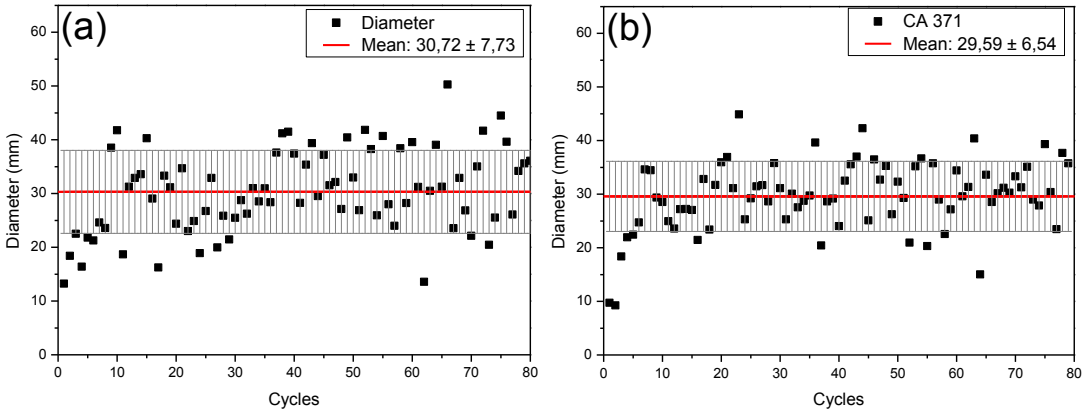

Figure 10. Diameter for the first 80 cycles of combustion versus cycles for fixed crank angle of 15 CA after ignition by lateral DI mode: a) G73E27; b) G100.

Analyzing the equivalent flame diameter for fixed angle (Fig 11), the central DI showed better results compared to the PFI and lateral DI modes. Higher mean was found the position of the injector in the center and with the increase in injection pressure provided less standard deviation and greater uniformity in the data. Due to the ascending diameter profile, mainly from cycle 40 on, it is believed that the average diameter will be larger under PTR conditions.

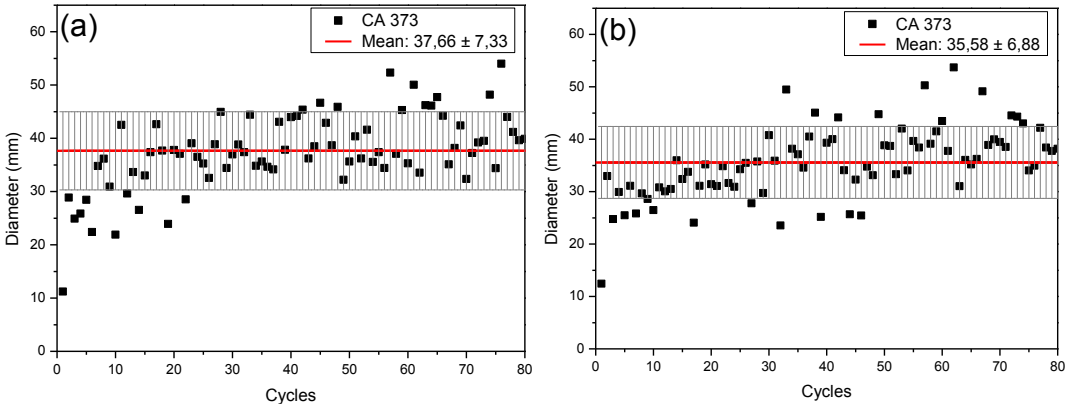

Figure 113. Diameter for first 80 combustion cycles versus fixed crank angle 15 CA cycle after ignition by central DI mode with G73E27 at: a) 150 bar and b) 200 bar.

The geometric center of the flame was analyzed for the first 80 combustion cycles at 10° CA after ignition, as shown in Figure 12. The geometric zero points are defined with the center of the combustion chamber and the spark plug is located 5 mm above the geometric center towards the exhaust valve. For PFI mode, the fuels showed little dispersion, highlighting the G73E27 with a little more variability due to the chemical characteristics of ethanol in the composition.

For the DI mode (Fig. 13), a greater displacement to the region of the exhaust valve is observed. This is due to the position of the injector, the high-temperature gradient in this region, and the characteristic tumble movement of the engine with greater intensity in the region of the exhaust valve (Abrantes, 2017 e Oliveira, 2017). In addition, the increased fuel penetration caused by direct injection into the chamber can contribute to more fuel located in this region. Despite good cycle uniformity, similar to PFI, the G73E27 shows greater variability compared to G100.

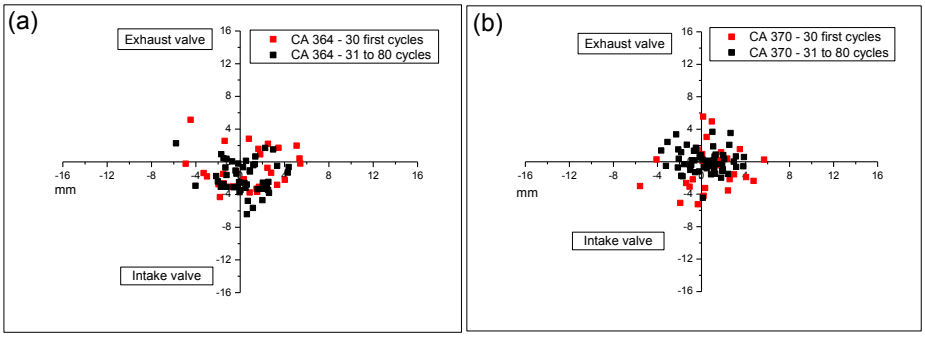

Figure 12. Image Center for first 80 combustion cycles after 10 crank angles after central DI mode ignition with: a) G73E27 and b) G100.

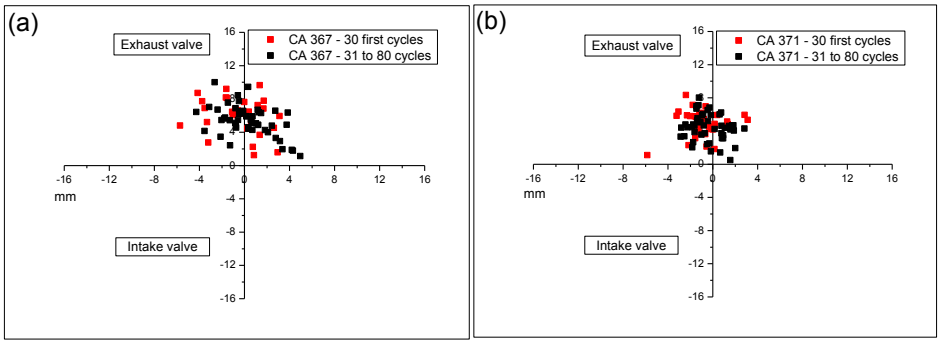

Figure 13. Image Center for first 80 combustion cycles after 15 crank angles after central DI mode ignition with: a) G73E27 and b) G100.

When applying the central ID injector, the behavior is similar to the lateral DI with the profile displaced to the exhaust valve for the same reason (Fig. 14). The increase in injection pressure provided a flame casing with more uniform growth and less spread. This observed profile is linked to higher combustion efficiency in terms of complete combustion due to better vaporization.

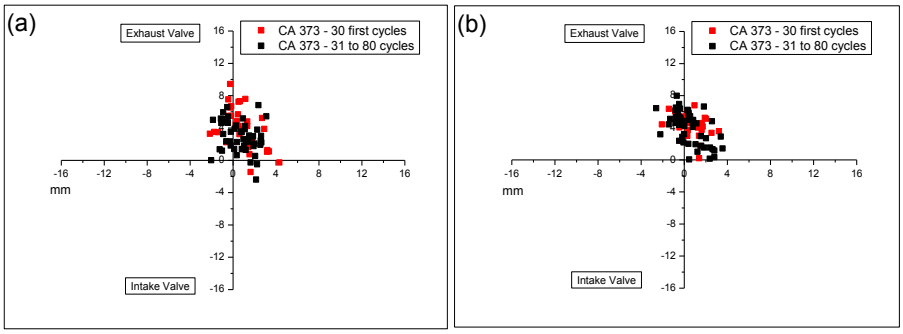

Figure 14. Image Center for first 80 combustion cycles after 15 crank angles after central DI mode ignition with E95W5 at: a) 150 bar and b) 200 bar.

In addition to the optical information, the thermodynamic data were analyzed to obtain an overview of the combustion process of the first cycles. In Figures 15 and 16, the maximum pressure signals in the cylinder for the first 80 combustion cycles are observed.

In PFI mode, for both fuels, the process starts presenting several ignition failures and incomplete combustion, the cylinder pressure signal presented only the peak of the motorized pressure signal. This effect is associated with temperature in the combustion chamber, the inefficiency of vaporization thus providing a very poor mixture. In addition, low-pressure injection into the inlet manifold at low temperature contributes to the inadequate formation of the air-fuel mixture. After this initial period, the valve, collector, and chamber wall tend to heat up and the pressure profile grows and with this, as the movement decreases the variability.

Also mirroring the optical information, the thermodynamic data from the direct injection mode show similar results. When observed the behavior between the injection modes, the DI model generates more expressive cylinder pressure results from the beginning of the process. Great variability and less chance of identifying the cycle in which combustion failures may occur are some of the characteristics of this injection mode. Once the start is overcome, lower variability and probability of no combustion are noted.

Large variations between consecutive cylinder pressures, as already discussed above, are due to the presence of non-vaporated fuel from the previous cycle which collaborates for richer mixtures in the next cycle. This characteristic tends to cause higher levels and emission of hydrocarbons and carbon monoxide.

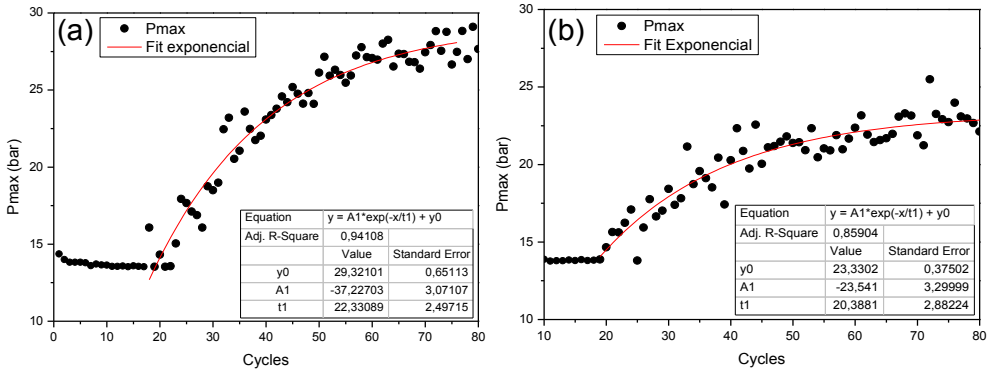

Figure 15. Maximum pressure (bar) vs cycles for the first 80 cycles by PFI: a) G73E27 and b) G100.

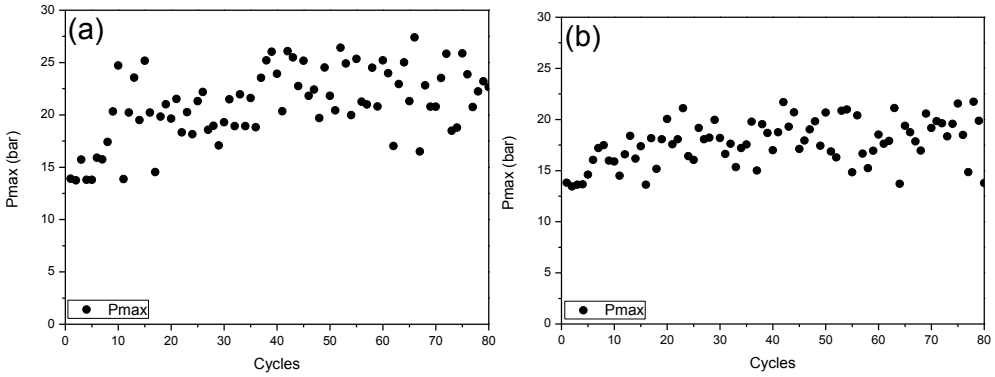

Figure 16. Maximum pressure (bar) vs cycles for the first 80 cycles by lateral DI: a) G73E27 and b) G100.

The increase in fuel injection pressure caused changes in cylinder pressure for the G73E27. Factors such as the decrease in droplet and the longer residence time of the fuel inside the chamber provided by the increase in injection pressure were factors I generated this improvement. Despite the greater uniformity of maximum pressures, the result was not very significant (Fig. 17). The time inside the cylinder and the size of the drops without the injection pressure increase already provided good combustion for the G73E27, due to the lower latent heat of vaporization. As a result, the increase in pressure represented little change. For other fuels with greater difficulty in vaporization, such as ethanol, this increase in pressure can generate much more significant results.

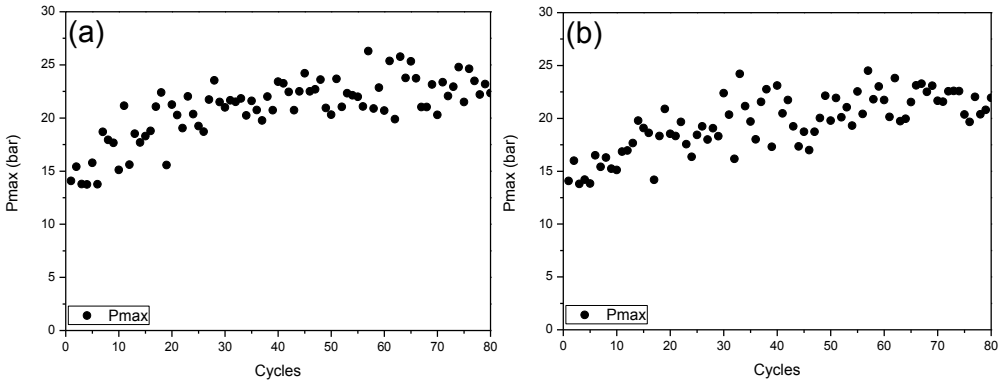

Figure 17. Maximum pressure (bar) vs cycles for the first 80 cycles by central mode DI: a) 150 bar and b) 200 bar.

Table 1. Maximum mean pressure, maximum value and coefficient of variation for lateral and central DI.

	G73E27 Lateral DI	G100 Lateral DI	G73E27 Central DI	G73E27 Central DI
Injection pressure [bar]	150	150	150	200
Pmax average [bar]	21.09	17,72	21.00	19.70
Maximum Pmax value [bar]	27.40	21,73	26,3	24.5
CvPmax [%]	16.1	12.4	13.8	13.7

Besides the cylinder pressure as thermodynamic information, evaluating the IMEP in Figs. 18 and 19, it is observed in the first cycles of PFI mode the presence of negative values in this initial interval for both fuels. This is due to the absence of combustion and poor burning, which the pressure transducer has difficulty measuring. After that, an increase in the value of IMEP is observed, in which the greatest variability is present in G73E27 due to the composition of the ethanol present, as previously discussed.

When observed the IMEP for DI mode, the faster response was obtained with both fuels. However, it can be seen that the presence of ethanol in the mixture and the low temperature in this initial period causes great variability throughout the process, which can lead to some cycles with results well below average. As the G73E27, possibly when the system has warmed up, it can be seen that the values have decreased the standard deviation considerably. The G100 due to its composition and advantages in this low-temperature period presents results with low variability throughout the process.

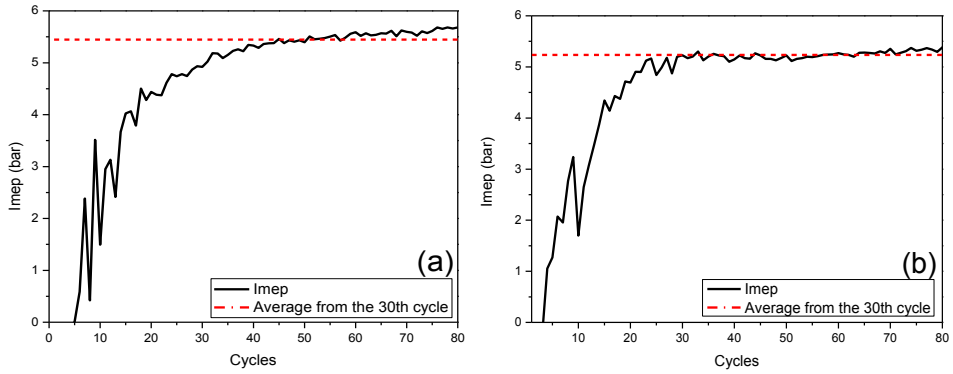

Figure 18. IMEP vs. cycles for first combustion cycles by PFI mode: a) G73E27; b) G100.

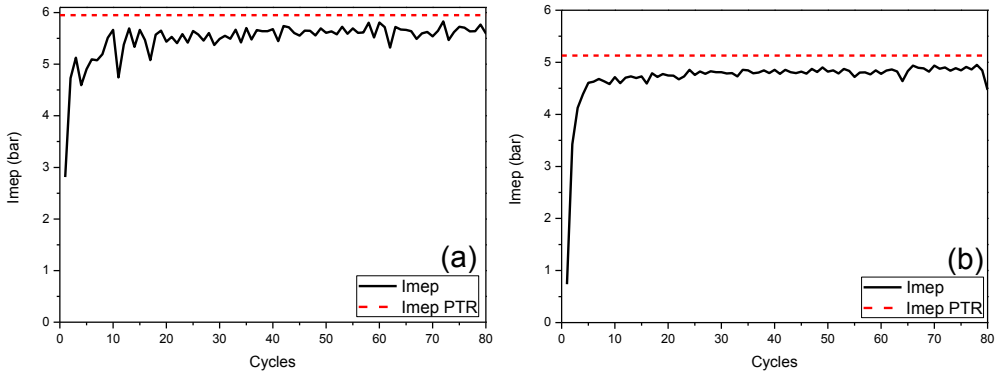

Figure 19. IMEP vs. cycles for first combustion cycles by lateral DI mode: a) G73E27; b) G100.

The IMEP values for the central DI are presented in Fig 20 and Table 2, where they show the good result of this mode of operation. Since the first cycles, results close to the average PTR and with uniformity without great variability. The increase in injection pressure caused lower CvIMEP values. Compared to other modes of operation, the central DI achieved much better results where in addition to higher IMEP, they provided lower CovIMEP for both 150 and 200 bar.

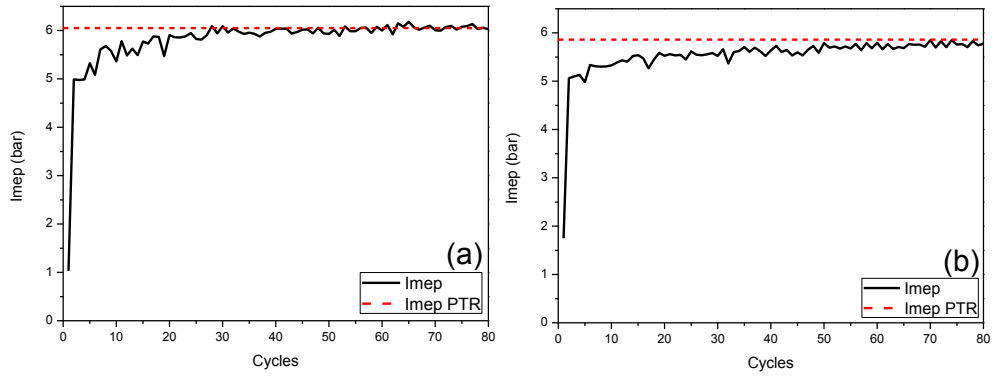

Figure 164. IMEP vs. cycles for the first combustion cycles by the central DI mode with G73E27: a) 150 bar; b) 200 bar.

Table 2. Average, minimum and coefficient of variation for PFI, lateral and central DI.

	G73E27 PFI	G100 PFI	G73E27 DI lateral	G100 DI lateral	G73E27 DI central	G73E27 DI central
Injection pressure [bar]	4.2	4.2	150	150	150	200
Average IMEP [bar]	5.45*	5,24*	5,49	4.71	5,83	5,55
Max IMEP [bar]	5.68*	5,38*	5.83	4.95	6,18	5,87
CvIMEP [%]	3.2*	1.3*	6.9	10.4	10,3	8,3

* Average IMEP, minimum and coefficient of variation for fuels assessed by PFI mode from cycle 30 onwards.

4. CONCLUSION

In this work, the behavior of the first combustion cycles for PFI injection mode, lateral DI, and central DI was analyzed from optical and thermodynamic data, demonstrating that optical information and its morphological analysis are an excellent research tool.

Due to the low temperature of the engine parts and the combustion chamber during the first combustion cycles, the adverse operation during this period causes the difficulty of evaporation of the fuel and this makes the air-fuel ratio inefficient. This behavior can lead to frequent ignition failures and incomplete combustion. The physical-chemical characteristics of fuels have an important factor in this process. The presence of ethanol in the blend due to its higher latent vaporization heat compared to gasoline may affect the difficulty of forming the vaporized mixture during this initial low-temperature period. As the combustion process progresses, the temperature tends to increase and the operation tends to the permanent thermal regime where the cyclical variations are smaller compared to the initial period.

When comparing the fuel injection modes, it was possible to observe in the PFI a profile of exponential growth of the flame front, with difficulties of formation in the initial period until it reached a stable period. In this period, 5 stages were identified in the development of combustion. At the first moment, inefficient vaporization due to the low

temperature in the intake manifold induces combustion failure and the absence of flame. In the second stage, the flame presents low development and energy release, however still in a very poor air-fuel mixture. In the third moment, better vaporization and consequently better-developed flame is observed. In the fourth stage, more stable propagation with less variability is observed. Finally, in the fifth stage, the fuel tends to achieve stability of the permanent thermal regime. The time of each stage depends on the physical and chemical characteristics of the fuel used. For the lateral DI mode, different from the PFI, expressive results are obtained since the beginning of the operation. Nevertheless, for the fuels studied, ignition failures and high variability were observed in thermodynamic responses.

When applied to the injection through the central DI mode, it was observed that the change in the position of the injector inside the chamber has a great influence on the burning behavior. Better fuel distribution and consequently less contact with the chamber walls still under low temperature provided better optical and thermodynamic results compared to lateral DI and PFI. In addition, the increase in injection pressure, which provides better atomization of the fuel, has also provided better results with faster responses and less cyclic variability in these initial cycles, showing itself to be an interesting strategy for solving such problems when using fuels with high vaporization heat such as ethanol.

5. ACKNOWLEDGEMENTS

This work was supported by LCPE-ITA and FAPESP-PSA.

6. REFERENCES

Abrates, T. T. da S. *Application of the PIV technique in an internal combustion engine with optical access to study the Tumble and Swirl phenomena*. [s.l.] (text in portuguese), Instituto Tecnológico de Aeronáutica, 2017.

Augoye, A. and Aleiferis, P., 2014. "Characterization of Flame Development with Hydrous and Anhydrous Ethanol Fuels in a Spark-Ignition Engine with Direct Injection and Port Injection Systems". *SAE Technical Paper* 2014-01-2623, doi:10.4271/2014-01-2623.

Augoye, A.; Aleiferis, P. Characterization of Flame Development with Hydrous and Anhydrous Ethanol Fuels in a Spark-Ignition Engine with Direct Injection and Port Injection Systems. *SAE Technical Paper*, v. 01, n. 2623, 2015.

Awad, O. I. et al. Alcohol and ether as alternative fuels in spark ignition engine: A review. *Renewable and Sustainable Energy Reviews*, v. 82, p. 2586–2605, 2018.

Baêta, J.; Pontoppidan, M.; Silva, T. Exploring the limits of a down-sized ethanol direct injection spark ignited engine in different configurations in order to replace high-displacement gasoline engines. *Energy Conversion and Management*, v. 105, p. 858–871, 2015.

Catapano, F.; Sementa, P.; Vaglieco, B. M. Optical characterization of bio-ethanol injection and combustion in a small DISI engine for two wheels vehicles. *Fuel*, v. 106, p. 651–666, 2013.

Costa, R. et al. E100 Stratified Lean Combustion Analysis in a Wall-Air Guided Type GDI Optical Engine. *SAE Technical Paper*, p. 1–9, 2015.

Di Iorio, S.; Sementa, P.; Vaglieco, B. Experimental Characterization of an Ethanol DI - Gasoline PFI and Gasoline DI - Gasoline PFI Dual Fuel Small Displacement SI Engine. *SAE Technical Paper*, p. 1–8, 2015.

Fan, Q.; Li, L. Study on first-cycle combustion and emissions during cold start in a TSDI gasoline engine. *Fuel*, v. 103, p. 473–479, 2013.

Hattori, F. Analysis of fuel and combustion behavior during cold starting of SI gasoline engine. *JSAE Review*, v. 18, n. 4, p. 351–359, 1997.

Heywood, J. B. *Internal Combustion Engine Fundamentals*. 1st ed. New York, USA: McGraw-Hill, 1988.

Kumar G, S.; Kumar, G. Initial Development of a E85 Fueled, Multi Cylinder, Turbocharged, Spark Ignited, Heavy Duty Engine. *SAE Int. J. Engines*, v. 10, n. 1, p. 55–60, 2017.

Oliveira, S. A. L. *Spray Analysis in direct injection spark ignition engine using PIV technique*. [s.l.] Instituto Tecnológico de Aeronáutica, 2017.

Romero, C. A.; Mejia, L. A.; Carranza, Y. Influence of Ethanol Content, Compression Ratio and Cylinder Head Material on Idling Speed, Warm-Up Time and Emissions of a Non-Road Small Single Cylinder Gasoline Engine. *SAE Technical Paper*, p. 1–9, 2016.

Shahad, H. A. K.; Wabdan, S. K. Effect of Operating Conditions on Pollutants Concentration Emitted from a Spark Ignition Engine Fueled with Gasoline Bioethanol Blends. *Journal of Renewable Energy*, v. 2015, p. 1–7, 2015.

Trevas, I. et al. Combustion Analysis on a Variable Valve Actuation Spark Ignition Engine Operating with E22 and E100. *SAE Technical Paper*, p. 1–12, 2017.

Waqas, M. et al. Blending octane number of ethanol in HCCI, SI and CI combustion modes. *SAE International Journal of Fuels and Lubricants*, v. 9, n. 3, p. 659–682, 2016.

Yang, Y. et al. Understanding fuel anti-knock performances in modern SI engines using fundamental HCCI experiments. *Combustion and Flame*, v. 162, p. 4008–4015, 2015.

Zhuang, Y.; Hong, G. Primary investigation to leveraging effect of using ethanol fuel on reducing gasoline fuel consumption. *Fuel*, v. 105, p. 425–431, 2013.

Zhang, S. et al. Cold starting characteristics analysis of hydraulic free piston engine. *Energy*, v. 119, p. 879–886, 2017.

7. RESPONSIBILITY NOTICE

The author(s) is (are) the only responsible for the printed material included in this paper.